Materials Advances

ROYAL SOCIETY OF CHEMISTRY

PAPER

View Article Online
View Journal | View Issue

Cite this: *Mater. Adv.*, 2024, 5, 9314

Sodium alginate-nanocellulose-based active composite film for edible oils packaging applications†

Sazzadur Rahman,[a] Chandramani Batsh,[a] Shalini Gurumayam,[b] Jagat Chandra Borah[b] and Devasish Chowdhury *[a]

Edible oils are prone to spoilage through aerial oxidation, leading to a reduction in their shelf life. In this study, we developed a nanocomposite biopolymer film designed for packaging edible oils. To enhance the antioxidant properties of the film, an extract from *Moringa oleifera* plants was obtained through solvent extraction and incorporated into the biopolymer. This infusion of plant extract bestowed antioxidant characteristics upon the resulting material. It was determined by GC–MS that *Moringa oleifera* water extract contains 9-octadecenamide, (*Z*)-(an Oleamide), which provides antioxidant properties. Additionally, cellulose nanofibers (CNF) were extracted from *Terminalia arjuna* plant fruits using the acid hydrolysis method. These CNFs were further introduced into the biopolymer to reinforce its mechanical properties of the biopolymer. The stability of the biopolymer film was evaluated in various edible oils (*viz.* mustard oil, olive oil, soybean oil, and sunflower oil), and the optimized nanocomposite film exhibited a tensile strength of approximately 44 MPa in the dry state. The antioxidant capacity was assessed using DPPH (2,2-diphenyl-1-picrylhydrazyl) and ABTS (2,2′-azina-bis(3-ethylbenzothiazoline-6-sulfonic acid)) free radical scavenging assays. The plant extract-based biopolymer nanocomposite film, specifically the (0.25CNF-4WME-SA) formulation, demonstrated the highest antioxidant activity, reaching 60.55% and 41.33% against ABTS and DPPH, respectively. The practical effectiveness of the 0.25CNF-4WME-SA film was further demonstrated through its application in packaging edible oil, showcasing its ability to scavenge free radicals generated during the storage of edible oil. The cytotoxicity of the fabricated film was evaluated using CC1 hepatocyte cells as an *in vitro* model. The developed nanocomposite material, incorporating plant extract, holds promise as an active packaging material for edible oils.

Received 1st July 2024,
Accepted 27th October 2024

DOI: 10.1039/d4ma00670d

rsc.li/materials-advances

1. Introduction

One of the most popular foods in the human diet is edible oil, which is becoming more acknowledged for its importance to human health, nutrition, and the food industry.[1] More than 90% of oils originate in plants, animals, or marine environments.[2] The most popular edible oils used globally as a human cooking medium and in the food industry are sunflower, olive, mustard, and soybean oils. One crucial chemical process that causes concern in the food sector is lipid oxidation. It causes food products to lose nutritional content and have a shorter shelf life at different stages, such as during storage, processing, shipping, and final manufacture for consumers. Inevitably, such oxidation reactions can occur to both primary and secondary naturally occurring components in oils, reducing their quality and forming many oxidized compounds. Therefore, it is imperative to slow down or prevent these reactions to maintain the quality of edible oils and food products. Antioxidants can be considered an economical and effective way to protect edible oils against oxidation.[3] Synthetic antioxidants like butylated hydroxyanisole, butylated hydroxytoluene, and tertiary butyl hydroquinone are commonly employed in the food industry due to their robust effects, affordability, stability, and widespread availability. Research has shown that artificial antioxidants are highly hazardous, carcinogenic, and may even damage the liver.[4] Thus, on a larger scale, natural antioxidants derived from plants remain a key area of research, especially when sourced from affordable, abundant, and environmentally sustainable materials. The *Moringa*

[a] *Material Nanochemistry Laboratory, Physical Sciences Division, Institute of Advanced Study in Science and Technology, Paschim Boragaon, Garchuk, Guwahati 781035, India. E-mail: devasish@iasst.gov.in, srahman.ngn1994@gmail.com, student.chandramani@gmail.com; Fax: +91 361 2279909; Tel: +91 361 2912073*

[b] *Chemical Biology Lab1, Life Sciences Division, Institute of Advanced Study in Science and Technology, Paschim Boragaon, Garchuk, Guwahati 781035, India. E-mail: borahjc@gmail.com*

† Electronic supplementary information (ESI) available. See DOI: https://doi.org/10.1039/d4ma00670d

oleifera plant, renowned for its biological and nutritional significance, is recognized for its rich reservoir of antioxidant compounds. Widely cultivated in South Asia, this tree serves various purposes, exhibiting anti-cancer, anti-diabetic, anti-inflammatory, anti-microbial, and antioxidant properties.[5] It has been known that their leaves contain the highest amount of polyphenol groups, followed by flowers and seeds.[6] These polyphenols are responsible for the antioxidant activity. The water-based extract derived from *Moringa oleifera* leaves is rich in phenolic compounds and boasts the highest flavonoid content compared to other plant parts.[7] Moreover, extracting active compounds from plants using aqueous-based methods is highly cost-effective since water serves as an economical, secure, and readily available solvent.[8] Recently, Giulia Barzan *et al.* developed an eco-friendly cellulose-based active packaging material by utilizing food-industry waste and incorporating extracts from Moringa leaves as antioxidant agents. They exhibited a notable *in vitro* free radical defence (with an antioxidant potency of 50%) and effectively hindered ground beef lipid peroxidation by over 50% throughout a 16-day duration.[9]

Traditionally, edible oils are stored in glass, metal and plastic films made from polyethylene terephthalate. In addition, polyethylene terephthalate has favourable mechanical properties and low gas permeability, shielding edible oils from gas exposure and is notably lighter than glass.[10] However, the extensive use of polyethylene terephthalate bottles contributes significantly to waste generation, causing a threat to the environment. In 2018, global plastic production reached a staggering 359 million tons, with only about one-third of it being recycled. The net demand for polyethylene terephthalate in the EU27 + UK was estimated at 5.1 million tons in 2020, with 3.0 million tons originating from virgin polyethylene terephthalate production and 1.3 million tons from recycled polyethylene terephthalate production. Polyethylene terephthalate has a prolonged environmental degradation rate, with the potential to persist for up to 2000 years. Given these environmental concerns, ongoing efforts are being made to explore alternative packaging materials. Biopolymers-based material is the only green alternative to single-use plastic materials. Biopolymers are natural polymers produced by natural resources and are biologically renewable, biodegradable, biocompatible, and non-toxic materials.[11,12]

Alginic acid is a naturally occurring edible polysaccharide found in brown algae in the ocean.[13] It is hydrophilic and forms a viscous gum when hydrated. It has gained extensive use as a material for food packaging because of its ability to synthesize film.[14] An advantage of seaweed-based biopolymers lies in their abundant availability, as they can be cultivated beneath the ocean. This, in turn, conserves land for alternative agricultural purposes and contributes to mitigating environmental carbon emissions. Alginate, a frequently employed biopolymer derived from seaweed, is a copolymer comprising (1–4) linked β-D-mannuronic acid (M) and α-L-guluronic acid (G) groups.[15,16] However, sodium alginate (SA) has film-forming properties but has low mechanical strength and poor gas permeability. Blending with other polymers, cross-linking, and incorporation of nanofillers have been used to improve such drawbacks.[17]

Cellulose nanofiber (CNF) emerges as a promising material, serving as a sustainable reinforcement for the development of high-performance biocomposite materials. This is due to their numerous advantages, which include nanoscale dimensions, high aspect ratios, low densities, cost-effectiveness, and high biodegradability.[18] These exceptional mechanical properties also extend to the resultant nanocomposites.[19] Cellulose is the primary and most plentiful renewable polysaccharide found in both plants and microorganisms.[20] The extractions of the CNF are usually used from naturally abundant plant sources such as leaves, tough fibres, seeds, fruits, wood, cereal straws, and other grass fibres.[21] CNFs can be produced by using physical, chemical, biological, and oxidation techniques from the cellulose-containing materials. In chemical methods, cellulose nanofibers are synthesized through acid hydrolysis, which breaks down the amorphous regions of the fibres to yield nanocrystalline nanofibers.[20]

Arjuna, scientifically known as *Terminalia arjuna*, is a tree reaching heights of 40–60 feet and is found native to India's sub-Himalayan, central, and southern regions. This tree holds significant importance in various traditional medicinal systems, including Unani, Ayurveda, Tibetan, and Homeopathy.[22] The fruit, characterized by its fibrous and woody texture, has dimensions of 4–5 cm in length and 2–3 cm in width. Its color undergoes a transformation from green to yellow, culminating in a ripening stage marked by a brown hue.[23] Generally, people discard or incinerate a significant amount of arjuna fruits in every year.[24] In this report, CNF was synthesized from the ripe fruits of *Terminalia arjuna* by using acid hydrolysis. Although the *Terminalia arjuna* plant fruits are well documented for use as a medicinal application in the literature,[25] however, to the best of our knowledge, till now, there is no report of publications devoted to the synthesis of CNF from the *Terminalia arjuna* plant fruits.

In this study, an antioxidant-active nanocomposite film was developed to extend the shelf life of edible oil. For the first time, CNFs were extracted from ripe *Terminalia arjuna* fruits through acid hydrolysis, offering a sustainable approach by transforming waste into a valuable resource. This approach aligns with circular economy principles, contributing to sustainable practices. The synthesized CNF was incorporated into SA biopolymer to enhance its mechanical and antioxidant properties. Additionally, an aqueous extract from *Moringa oleifera* leaves was incorporated into the nanocomposite, imparting antioxidant properties. The antioxidant property of the fabricated nanocomposite film was assessed using DPPH and ABTS free radical scavenging assays. A practical demonstration of edible oil packaging with antioxidant properties is studied in details. This study successfully demonstrates the development of an antioxidant-active nanocomposite film that can extend the shelf life of edible oil.

2. Materials

Leaves of *Moringa oleifera* (Moringa) are collected from the IASST, Guwahati Campus. Sunflower, soybean, mustard, and olive oils are purchased from the Boragaon market in Guwahati,

India. Sodium Alginate is obtained from Merck. DPPH (2,2-diphenyl-1-picrylhydrazyl) molar weight 394.32 (extrapure) is procured from SRL Chemicals, India. ABTS [2,2′-azina-bis(3-ethylbenzothiazoline-6-sulfonic acid)] molecular weight 548.68 (extrapure) is procured from SRL Chemicals, India. Sodium hydroxide (NaOH), hydrogen peroxide (H_2O_2), sulphuric acid (H_2SO_4), chloroform and acetic acid (CH_3COOH) were obtained from Sigma-Aldrich, India. All the chemicals were used without any further purification.

3. Methods

3.1. Preparation of cellulose nanofibre

The synthesis procedure of cellulose nanofibre is given in Scheme 1(a). Briefly, the ripe fruits of *Terminalia arjuna* were collected from the IASST campus. The fruits were washed with tap water 2–3 times to remove dust and other organic matter, then washed with distilled water 2–3 times. The cleaned fruits were dried using a hot air oven at 60 °C for 24 h. The dried and cleaned fibrous pulp of the fruits was ground using a kitchen grinder. By using a mesh of size 120 μm, the uniformly sized ground powder was collected. 2 grams of dried Arjuna plant fruit powder (AFP) were taken and washed with distilled water using a magnetic stirrer for 2 h at 60 °C. This process was repeated 1–2 times. The washed powder was dried in a hot air oven for 6–8 h at 60 °C. The dried powder was collected and stored at 4 °C for further treatment. The powder was subjected to alkali treatment (2% NaOH) to remove lignin from the dried AFP. The dried powder was stirred in a 100 mL solution of 2% NaOH using a magnetic stirrer for 2 h at 80 °C, and this process was repeated once more. The resulting solution was filtered through Whatman no. 1 filter paper and washed with distilled water multiple times until a neutral pH was achieved. Subsequently, the extract was dried in a hot air oven for 24 h at 60 °C. To remove any remaining soluble impurities, the dried extract was bleached by stirring with 100 mL of 6% hydrogen peroxide (H_2O_2) using a magnetic stirrer for 90 minutes at 60 °C. A few drops of glacial acetic acid are added during the process to enhance the bleaching efficiency. For better results, the extract is bleached twice. The solution was then filtered and washed with distilled water several times until the neutral pH was reached. The bleached material was dried in a hot air oven at 60 °C for 24 h. The resulting dried sample underwent acid hydrolysis in a round bottom flask, using a 40% H_2SO_4 solution, maintained at 45 °C for 2 h. The solution is now kept untouched until the temperature reaches room temperature. Filter the supernatant and rinse it with distilled water until it attains a neutral pH. The resulting product is cellulose nanofibres, and it is labelled as CNF.

3.2. Preparation of moringa leaf extract

The *Moringa oleifera* leaf extract synthesis procedure is given in Scheme 1(b). The fresh leaves of *Moringa oleifera* plant were collected from the IASST campus. The leaves were washed with distilled water several times to remove dust and other water-soluble impurities. The washed leaves were dried in a hot air oven at 50 °C for 12 h. The dried leaves were ground into a fine powder with a kitchen grinder. About 8 g of dried powder was subjected to 80 mL of water in a glass beaker. The solution mixture was stirred using a magnetic stir for 4 h at RT and then kept untouched overnight. The solution was centrifuged for 30 minutes at 7870 rpm to get the supernatant. This process was repeated once more to remove the large particles associated with the supernatant. The supernatant was collected, and the solvent was evaporated from the extract using a rotary evaporator. The plant extract was kept in the −4 °C refrigerator for further use. The extract was labelled as WME.

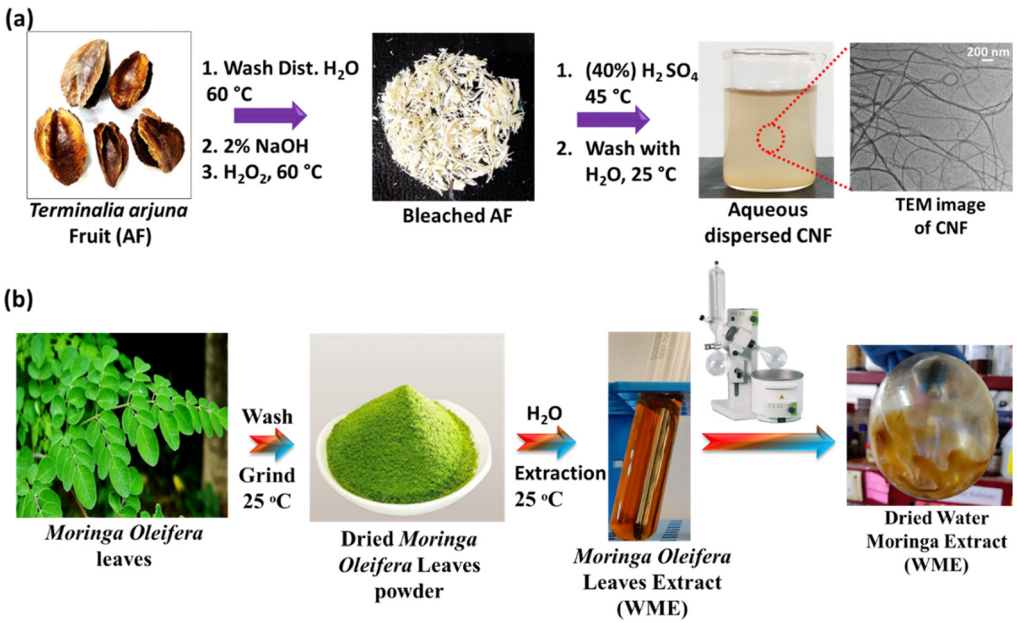

Scheme 1 (a) Synthesis of cellulose nanofibre (CNF); (b) extraction of Moringa extract from water (WME).

3.3. Synthesis of SA film

0.8 g of SA was dispersed in 60 mL of water and stirred at 600 rpm with a magnetic needle using a magnetic stir at RT. The resulting homogeneous solution was degassed by using sonication. After degassing, a 30 mL solution was cast on a polypropylene Petri dish with a diameter of 9 cm. The biopolymer casted Petri dish was subjected to a hot air oven and dried at 55 °C. The dried biopolymer was peeled out gently and stored in a vacuum desiccator for further characterization. The blank fabricated film was labelled as SA film.

3.4. Synthesis of SA-WME film

Different percentages of WME containing SA film were fabricated by varying the percentage of WME with respect to the total weight of the biopolymer (0.8 g). For this, the plant extract was taken at different percentages, such as 1%, 4%, 8%, and 12% (w/w) with respect to the total weight of SA and dispersed in 10 mL water in the different beakers. Each percentage of 10 mL plant extract was added into the 50 mL of 0.8 g aqueous dispersed SA homogeneous solution in the different glass beakers. The 50 mL of 0.8 g aqueous dispersed SA homogeneous solution was prepared following the procedure discussed in Section 3.3. However, here, 0.8 g of SA was dispersed into 50 mL of water.

The different percentages of plant extract were stirred evenly in a magnetic stirrer for 12 h to make a homogeneous mixture. Each homogeneous mixture was sonicated to degas and remove the air inside the solution to make the film bubble-free. Each solution was cast on a polypropylene Petri dish (30 mL solution in each) and kept in a hot air oven at 55 °C to dry completely. Each dried film was peeled out and stored in a vacuum desiccator for further characterization. The composite film prepared by taking the percentage of WME such as 1%, 4%, 8%, and 12% (w/w) was labelled as 1WME-SA, 4WME-SA, 8WME-SA, and 12WME-SA, respectively.

3.5. Synthesis of CNF-SA film

Initially, 0.8 g of SA was dispersed in 50 mL of water and stirred at 600 rpm using a magnetic stirrer at RT to form a homogeneous solution. To assess the optimal blending compositions of CNF with SA, various weight percentages of CNF (w/w) relative to the total weight of SA were blended into the SA biopolymer, resulting in a series of nanocomposite films. Different weight percentages of CNF (0.12%, 0.25%, 0.50%, 1%, 2%, and 4% w/w) were dispersed in 10 mL of distilled water in separate beakers. The CNF-dispersed solutions were added to the SA solution and stirred overnight until a homogeneous solution was achieved. Subsequently, the solution mixture underwent degasification using a bath sonicator to eliminate air and ensure a bubble-free film. Each solution mixture was cast over a polypropylene Petri dish with a volume of 30 mL and dried in a hot air oven at 55 °C. After complete drying, the film was allowed to attain room temperature, gently peeled off, and stored in a vacuum desiccator for further characterization. The composite films, prepared by blending SA with CNF at various percentages (w/w) such as 0.12%, 0.25%, 1%, and 4%, were labelled as 0.12CNF-SA, 0.25CNF-SA, 1CNF-SA, and 4CNF-SA, respectively (Table 1).

Table 1 Sample codes for the prepared films and their composition

S. no.	Sample code	Sodium alginate (SA) (g)	Moringa leaf extract (WME) (% w/w)	Cellulose nanofibers (CNF) (% w/w)
1	1WME-SA	0.8	1	NIL
2	4WME-SA	0.8	4	NIL
3	8WME-SA	0.8	8	NIL
4	12WME-SA	0.8	12	NIL
5	0.12CNF-SA	0.8	NIL	0.12
6	0.25CNF-SA	0.8	NIL	0.25
7	1CNF-SA	0.8	NIL	1
8	4CNF-SA	0.8	NIL	4
9	0.25CNF-4WME-SA	0.8	4	0.25

3.6. Synthesis of CNF-WME-SA film

The synthesis procedure of CNF-WME-SA film was given in Scheme 2. Briefly, 0.8 g of SA was dispersed in 40 mL of water by stirring using a magnetic stir at RT. 0.25% (w/w) of CNF and 4% (w/w) of WME, relative to the total amount of SA, were separately dispersed in 10 mL of distilled water in two distinct beakers. Initially, 0.25% CNF solution was added to the SA solution, and the mixture was stirred for 6 h to make a homogeneous solution. Subsequently, a solution with a concentration of 4% (w/w) WME was added to the aforementioned mixture and stirred overnight to attain a homogeneous solution. The solution mixture was subjected to degasification using a bath sonicator to make the film bubble-free. The solution mixture was cast over a polypropylene Petri dish with a volume of 30 mL and dried in a hot air oven at 55 °C. The dried film was gently peeled out and stored in a vacuum desiccator. The synthesis composite film was labelled as 0.25CNF-4WME-SA.

4. Characterization

4.1. UV-Visible spectroscopy

UV-visible absorption data of the films were studied using a Shimadzu UV spectrophotometer UV-2600. The samples were scanned through a range of 200–800 nm wavelengths.

4.2. Attenuated total reflectance-Fourier transform infrared spectroscopy (ATR-FTIR)

The prepared films, AFP, and CNF, were characterized by ATR-FTIR spectrometry in the range of wavelength 500–4000 cm^{-1} for analysis of the different functional groups with the help of PerkinElmer FT-IR instrument.

4.3. Thermogravimetric analysis (TGA)

The thermal stability of the films was studied by a thermogravimetric analyzer (TGA) PerkinElmer 4000 instrument. The film sample was cut into small pieces. In each experiment, 5–10 mg of each film was used for the TGA analysis with temperatures ranging from 35 to 800 °C under a nitrogen flow rate of 20 mL min^{-1} at a heating rate of 10 °C min^{-1}.

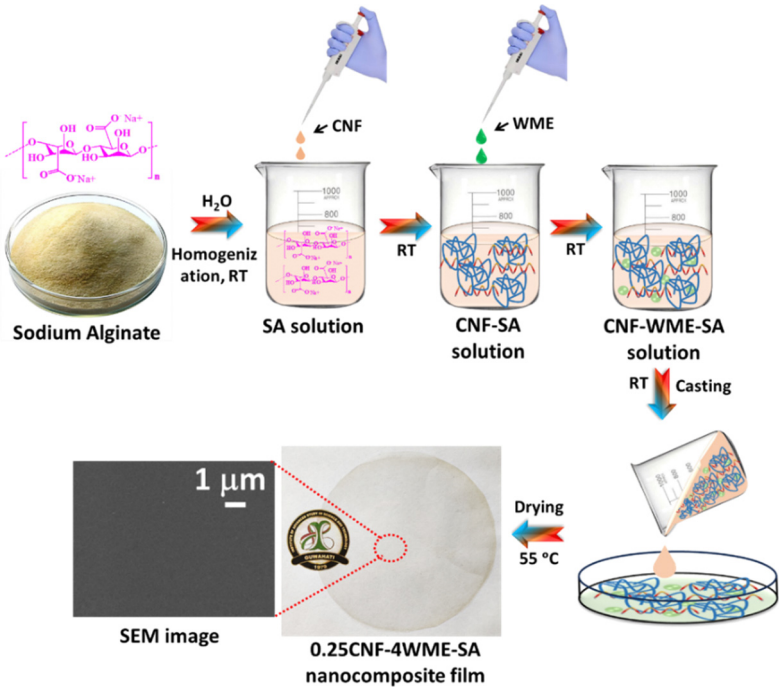

Scheme 2 Synthesis of biopolymer nanocomposite film.

4.4. X-Ray diffraction spectroscopy (XRD)

The X-ray diffraction (XRD) of the samples was collected by using a Bruker D8 Advance diffractometer instrument.

4.5. Scanning electron microscopy (SEM)

The surface morphology of the samples was studied using scanning electron microscope (SEM) (Carl Zeiss ∑igma VP' instrument).

4.6. Transmission electron microscopy (TEM)

Transmission electron microscopy (TEM) (JEOL TEM-2100) was used to study the morphology of the fabricated CNF.

4.7. Contact angle

The contact angle test is used to assess the wettability of a surface of biopolymer film. It measures the angle formed between the liquid droplet and the surface of the film when a droplet is placed on it. The contact angle was measured by using the instrument DSA 30E contact angle analyzer (Krüss GmbH, Hamburg, Germany).

4.8. Tensile strength

The mechanical properties of the films were studied by using a Tinius Olsen (model number H5KL) tensile machine and following the ASTM D638 standard. The testing was done by using a load cell of 5 kN and a speed of 5 mm min^{-1} at a gauge length of 10 mm. The experiment was conducted at room temperature. The samples were performed in triplicate.

4.9. Antioxidant activity

4.9.1 DPPH scavenging assay. In this, 0.1 mM DPPH solution was freshly made by dissolving dark-coloured DPPH powder (1.18 mg) into 30 mL of methanol and water solvent, respectively into amber colour vials as this reaction is a light-sensitive reaction. The mixture was left for 60 minutes at room temperature to produce free radicals. The DPPH absorbance was taken at 517 nm, which is the control. The film sample solution was prepared by dispersing 25 mg of film samples and dissolved completely in 5 mL of distilled water. From the solution, 1.2 mL of film sample solution was added into 4.0 mL of DPPH (0.1 mM) solution in a dark vessel and incubated for 60 minutes at RT. After 60 minutes, the absorption was taken for each sample at wavelength 517 nm using the photometric method. The samples were performed in triplicate. The radical scavenging activity was calculated using the following formula:

$$\text{DPPH inhibition (\%)} = (Ab_c - Ab_s)/Ab_c \times 100 \quad (1)$$

where Ab_c = absorbance value of DPPH solution at 517 nm; Ab_s = absorbance value of samples at 517 nm.

4.9.2 ABTS scavenging assay. ABTS scavenging assay was studied by following the procedure discussed by Das, P. *et al.*, with slight modifications.[26] In this, the 7 mM solution of ABTS was prepared in water. This solution is then mixed with 2.45 mM solution of potassium persulfate ($K_2S_2O_8$) on 1 : 1 volume ratio for 12 h. After that, the UV-visible spectra of this solution are taken at 735 nm in photometric mode, and the prepared solution is diluted till the absorbance of the solution comes to 0.7. This concentration, the final ABTS solution, is used for further treatment. 1.2 mL of sample solutions was added into the 4.0 mL of 7 mM ABTS solution and incubated for 5 minutes. The samples were performed in triplicate. The antioxidant activity of ABTS was determined using the following equation.

$$\text{ABTS inhibition (\%)} = (A_c - A_s)/A_c \times 100 \quad (2)$$

where A_c and A_s represent the absorbance of ABTS at around 735 nm in the absence and presence samples, respectively.

4.10. GC–MS spectroscopy

Gas chromatograph–mass spectrophotometer-TQ8030 equipped with EB-5 column and NIST library version was used to identify the compounds in WME. Helium gas served as the carrier gas, with a maintained flow rate of 1 mL min^{-1}. The injection port temperature was set at 280 °C, while the column oven temperature was at 50 °C with a hold time of 5 minutes. Subsequently, it was raised to 280 °C at a rate of 8 °C per minute, and the final hold duration was 29 minutes.

4.11. Water-vapor permeability (WVP)

The WVP tets evaluates the water vapour transmission rate through the polymer film. This experiment was performed following the ASTM E 96/E 96 M standard with slight modifications, as previously reported by our group.[13] The thickness of the film plays a pivotal role, and the thickness of the film was measured with the help of an electronic micrometre (Schut, Germany). The film thickness was measured randomly in six different places on each film, and the mean value was reported. The calculated thickness of the SA, 0.25CNF-SA, and 0.25CNF-4WME-SA film was 0.0044 cm, 0.0033 cm and 0.0044 cm, respectively. To conduct this experiment, initially, 20 g of calcium chloride was heated at 200 °C for 3 h in a Muffle Furnace. The dehydrated product was then placed in a vacuum desiccator until it reached room temperature. The dried calcium chloride was placed in a 100 mL glass beaker with a depth of 6.9 cm and a diameter 4.5 cm. Immediately, the beaker is mounted with the film sample tightly over the open surface of the beaker using cello tape so that the water vapour can enter or exit only through the film. The glass beaker is now kept in a closed glass desiccator to provide a 99% relative humidity environment. The glass beakers were weighed initially at $t = 0$ and after every hour for a period of 8 h ($t = 8$). The water vapour permeability (Unit = g cm cm^{-2} s^{-1} $mmHg^{-1}$) was calculated using the following equation,

$$\mathrm{WVP} = qd/ts\Delta p \quad (3)$$

where, q/t = slope of the weight increase *versus* time (g s^{-1}); d = composite film thickness (cm); s = area of the film which is exposed to moisture (15.89 cm^2); ΔP = difference of the vapor pressure between the two sides of composite films (23.76 mmHg).

4.12. Oil stability study of the biopolymer film

This test for biopolymer films assesses how the films retain their structural integrity and properties when exposed to oils. The test involves immersing the biopolymer film in the specific oil and observing change over time. Initially, strips of film samples of width 1 cm and length 8 cm were cut, and the strips were immersed into different edible oils for 24 h. The soaked film strips were collected from the edible oil, and the excess oil was removed from the film surface by using blotting paper. Finally, the tensile strength of the edible oil-treated sample was recorded. Here, we tested the stability of the film sample in different edible oils like sunflower, mustard, soybean, and olive oil.

4.13. Oil permeability

An oil permeability test for a biopolymer film involves measuring the rate at which oil molecules pass through the film. This test helps evaluate the film's barrier properties and suitability for oil packaging. 5 mL of edible oil was introduced into a test tube, and the open surface was tightly sealed with the biopolymer film. The sealed test tube was then inverted, with a filter paper placed beneath it. Initially, the weight of the dried filter paper was recorded. The system was left undisturbed for 24 h, and after this period, the weight of the filter paper was measured again. The oil permeability of the film sample was determined using the following equation.

$$P^{\circ} = (\Delta W \times \mathrm{FT})/(S \times T) \quad (4)$$

where, P° is oil permeability coefficient (g mm m^{-2} day^{-1}), ΔW is difference in weight of filter paper (g), FT is film thickness (mm), S is the exposed area of the film (m^2), T is incubation time (day).

4.14. Cytocompatibility study of the sample

4.14.1. Cell culture and maintenance. CC1 primary rodent hepatocytes were cultured in low glucose DMEM supplemented with 10% FBS and 1% antibiotic–antimycotic solution in 96 well plates and incubated till 80–90% confluency in a humidified 5% CO_2 incubator at 37 °C. Upon reaching the desired confluency, the cells were given fresh media and treated with SA, 0.25CNF-SA, and 0.25CNF-4WME-SA with dose with 125 μg mL^{-1} (diluted from a stock concentration of 1 mg mL^{-1} made in distilled filtered water as vehicle control). The control group was also treated with vehicle control. After 24 h of incubation, the media was discarded and replaced with 5 μM of resazurin solution and incubated for 4 h in CO_2 incubator. After 4 h, OD was measured at 570 and 600 nm wavelengths.

4.15. Edible oil packaging

A packaging experiment was carried out using soybean oil to assess the practical effectiveness of the 0.25CNF-4WME-SA film in prolonging the shelf life of edible oil. The packaging process involved placing 5 g of soybean oil into one open-ended glass tube. The diameter of open-ended glass tube is 3 cm. The glass tube containing oil was tightly mounted and sealed with the 0.25CNF-4WME-SA film. Subsequently, the sealed glass tube was inverted. A schematic depiction of the oil packaging process is provided in Fig. 6(b). To expedite storage tests, the inverted glass tube containing soybean oil was placed in an environmental chamber maintained at 50 ± 4 °C and 42 ± 2% relative humidity (RH) for a duration of 7 days. Additionally, a fresh 5 g sample of oil without packaging with active film was kept under the same environmental conditions as a control. Control sample was used for a comparison of peroxide values between the packaged oil and the control sample.

4.16. Peroxide value (PV)

The PV was determined according to the procedure R. Rashid *et al.*[4] Briefly, a 5 g oil sample was mixed with a total volume of 30 mL, consisting of chloroform and glacial acetic acid in a ratio of 2 : 3. To this mixture, 0.5 mL of saturated potassium iodide solution was added, and the resulting solution was thoroughly mixed. The reaction was allowed to proceed in dark conditions for 30 minutes. After the incubation period, the free iodine content was titrated against a 0.1 N sodium thiosulphate solution. During the titration, 1 mL of 1% starch solution was used as an indicator. The PV of the soybean oil was measured at the initial (fresh oil) and after 7 days of storage. The peroxide value expressed as mEq of oxygen per kg of oil was estimated by using the equation below:

$$\text{Peroxide value} = (A - B) \times W \times N \quad (5)$$

where B = volume of sodium thiosulphate used for blank, A = volume of sodium thiosulphate consumed by oil sample, W = weight of sample, N = normality of standard sodium thiosulphate.

4.17. Biodegradability test

The biodegradability of the composite films was assessed using a method adapted from Rahman *et al.*, with some modifications.[15] Samples, cut into 2 × 2 cm^2 pieces, were first dried in a hot air oven at 55 °C for 24 h to achieve a constant weight. These dried samples were then buried 5 cm deep in compost-containing garden soil placed in 500 mL glass beakers and kept at room temperature (~25 °C). Soil humidity was maintained at approximately 60% by sprinkling water. At specified intervals—4, 8, 12 and 16 days—the samples were removed from the soil, cleaned with 70% ethanol, and dried again in a hot air oven for 24 h. The experiment was carried out in triplicate.

5. Result and discussion

A highly edible oils stable active biopolymer film was fabricated by blending SA with CNF and WME plant extract using the solvent casting method. The CNF was fabricated from arjuna plant fruit by acid hydrolysis. The synthesized CNF was incorporated into the SA biopolymer solution by varying the amount (wt%) of CNF with respect to the total weight of SA (0.8 g). CNF was used as a reinforcing material for the fabricated active biopolymer. Variations in the blending percentage of CNF were carried out to optimize a suitable CNF composition that binds effectively with the biopolymer. We used 0.12%, 0.25%, 1%, and 4% of CNF and blended them with SA to make a different biopolymer nanocomposite film. These fabricated nanocomposites were labelled as 0.12CNF-SA, 0.25CNF-SA, 1CNF-SA, and 4CNF-SA, respectively. Among all the fabricated biopolymer nanocomposite films, the 0.25CNF-SA film shows excellent mechanical properties. To introduce the active property into the nanocomposite film, we incorporate WME extract. The WME extract was extracted from the *Moringa oleifera* leaf by using water as a solvent. The antioxidant property of WME extracts was studied using an ABTS and DPPH assay. To optimise the best formulation compositions of WME into biopolymer, different percentages of WME were added into the 0.25CNF-SA composite film. Finally, the antioxidant properties of the WME-biopolymer nanocomposite film were studied using both ABTS and DPPH assay. We incorporated 1%, 4%, 8%, and 12% (wt%) of WME into the SA biopolymer film and labelled them as 0.25CNF-1WME-SA, 0.25CNF-4WME-SA, 0.25CNF-8WME-SA, and 0.25CNF-12WME-SA respectively. Among them, 0.25CNF-4WME-SA nanocomposite film shows superior properties.

Pure SA film is not very stable in commonly used edible oils such as mustard, sunflower, olive, and soybean oil and also has poor mechanical properties. Therefore, blending a nanofiller such as CNF into SA improves the biopolymer composite film. Here, the CNF was fabricated from the arjuna plant fruit by acid hydrolysis. The synthesis procedure is discussed in the materials and method section. The cleaned raw arjuna plant fruit powder was bleached with H_2O_2 (6% v/v) to remove the plant pigments and physically attached dirty material from the powder. After that, to remove the chitin and hemicellulose material, the bleached powder was treated with the 2% (wt%) NaOH solution at 60 °C, and then adjusted the pH to neutral. The alkali-treated powder was subjected to acid hydrolysis to break the long bundles of cellulose chins and convert them into the nano form. The amorphous region of the cellulose was hydrolyzed and converted into nanofiber. The morphology of the fabricated CNF was characterized by TEM analysis. The TEM image of the CNF is given in Fig. 1(a). The TEM image showed that the CNF was a long fibrous structure with a length in the micrometre range and a calculated diameter of 22.42 ± 7.44 nm, confirming the nanofiber formation. The diameter was calculated using Image J software by taking the diameter of 50 different positions from the TEM image (Fig. 1(a)). The average size (diameter) distribution curve of the CNF is given in Fig. 1(b).

The functional group associated with the CNF and raw AFP was determined using FT-IR spectroscopy analysis in ATR mode, as shown in Fig. 1(c). The FT-IR peak for both AFP and CNF was observed at ~3340 cm^{-1}, illustrating the presence of a hydroxyl group due to –OH stretching frequency.[27] The peak at ~2900 cm^{-1} is due to the C–H symmetrical stretching present in both the CNF and AFP. In the AFP, peaks at 1728 cm^{-1} and 1632 cm^{-1} are attributable to the ester linkage of the carboxylic groups of lignin and carbonyl groups associated with the hemicellulose.[28,29] After chemical treatment during the formation of CNF, 1728 cm^{-1} and 1632 cm^{-1} peaks disappear as shown in Fig. 1(c). This suggests the removal of the hemicellulose and lignin in the CNF.[30] The peak at 1237 cm^{-1} corresponds to C=O stretching (guaiacyl ring) in the AFP, which is disappearance in the CNF because the elimination of lignin confirms that after acid hydrolysis, all these are eliminated, and there is only cellulose left.[31] Peak at ~1030 cm^{-1} corresponds to C–O stretching for glycosidic bonds, and 560 cm^{-1} corresponds to C–C bonds.[32]

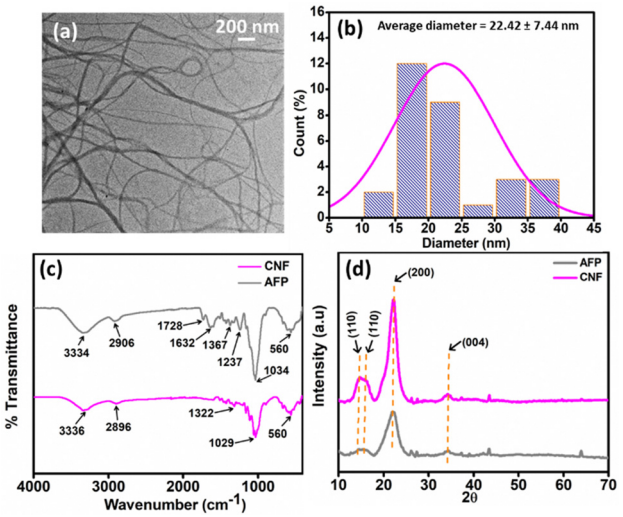

Fig. 1 (a) and (b) are the TEM image and diameter distribution curve of CNF; (c) and (d) are the ATR FT-IR and XRD spectra of CNF and AFP.

The XRD pattern of CNF and AFP are shown in Fig. 1(d). The four peaks at 2θ = 14.75°, 16.12°, 22.23° and 34.44° were observed, which corresponds to the crystal plan (110), (110), (200), and (004). These crystal planes are obvious for cellulose nanofiber[32] and correspond to the characteristic crystallographic plane of cellulose-I. The intensity of the crystalline peak at 22.23° was increased in CNF compared to the AFP. This occurs due to the increase in crystallinity after acid hydrolysis of AFP, and the crystalline structure of cellulose-I remains unchanged throughout the hydrolysis process.

5.1. Characterizations of biopolymer film

The FT-IR spectroscopy study was carried out on SA, 0.25CNF-SA, and 0.25CNF-4WME-SA films to identify their various functional groups and structural interactions, as shown in Fig. 2(a). In all the samples, a broad stretching observed near 3269 cm^{-1} was the characteristic peak due to the O–H stretching.[33] The band near 2922 cm^{-1} is mainly due to C–H symmetrical stretching. The peak near 1594 cm^{-1} stretching is typical of sodium alginate and representative of C═O stretching vibrations.[34] The peak near 1408 cm^{-1} and 1285 cm^{-1} is due to –COO– symmetric stretching and skeletal vibrations of the pyranose ring of alginate.[35] The bend observed around 1024 cm^{-1} can be attributed to the symmetric stretching vibrations of the C–O–C groups.[36] All the necessary peaks are found for all the fabricated films.

The percentage of light transmittance in packaging films could affect the rate of lipid oxidation caused by interactions between UV light and food.[37] A UV shielding packaging material is preferable for food packaging. Hence, UV-visible studies were carried out on SA, 0.25CNF-SA, and 0.25CNF-4WME-SA composite films. The UV spectrum of the composite films was conducted in transmittance mode through a range of 200–800 nm wavelength. The stacked UV spectrum of the samples is given in Fig. 2(b). It is evident from the stacked spectra % transmittance in the range of 200–400 nm is higher for blank film; however, after incorporations of WME, the UV transmittance was decreased. Such a decrease in UV transmittance is due to the absorption of UV light by the polyphenols groups inherently present in the WME. Polyphenols are known for UV light absorption properties.[38] The 0.25CNF-4WME-SA nanocomposite film sufficiently reduced UV transmittance as compared to the SA and 0.25CNF-SA film. Thus, the 0.25CNF-4WME-SA film can be used as UV shielding film in packaging applications.

Thermogravimetric analysis was performed on SA, 0.25CNF-SA and 4WME-0.25CNF-SA to study the thermal stability of fabricated films. The thermogram of the samples is given in Fig. 2(c). From the thermogram, it was found that there were three-stage degradation patterns in all films. The first stage of degradation starts at 35 °C and continues to 115 °C, with weight loss of about 7.20%. This occurs due to the evaporation of the physical contact water molecules with the film.[39] In the second stage, degradation of 0.25CNF-4WME-SA, 0.25CNF-SA, and SA film was started from 115 °C to 230 °C, 115 °C to 226 °C, and 115 °C to 224 °C respectively. During this degradation, the percent of weight loss was 5.90%, 5.41%, and 5.09% for the 0.25CNF-4WME-SA, 0.25CNF-SA, and SA film, respectively. The elevation of degradation temperature for the 0.25CNF-4WME-SA composite film as compared to the pristine film is due to the formation of intermolecular hydrogen bonding between the CNF, the polymer chains and the phenolic groups of WME. This degradation was mainly due to the breaking of interlinked functional groups. In the third step, the degradation in all the films started at 289.53 °C; there is a constant degradation of cellulosic material, plant extract, and raw sodium alginate, which caused constant decay.

The surface and cross-section morphology of the prepared biopolymer film were characterized using a scanning electron microscope (SEM). The SEM image of the surface and cross-sections of the films SA, 0.25CNF-SA, and 0.25CNF-4WME-SA are displayed in Fig. 3. The SEM image of the surface and cross-sections of the films 0.12CNF-SA, 1CNF-SA, and 4CNF-SA is displayed in Fig. S1 (ESI†). The pristine SA film surface microstructure was smooth, homogeneous, and without any cracks. However, upon the inclusion of 0.12% CNF, the film's surface became rough, and some cracks were noticeable in the cross-sections (Fig. S1d and d′, ESI†).

This could be attributed to the relatively weak interactions between the CNF and the polymeric chains. Moreover, in the 0.25% CNF blended film, the surface and cross-section microstructure became smoother and homogeneous with a continuous structure. This might be due to the good bonding interactions between the functional groups of CNF and polymeric chains of SA. With the increasing percentage of CNF 1% and 4%, the films become rough and start agglomerations of CNF in the biopolymer matrix. A phase separation was observed in the cross-section of the higher percentage of CNF nanocomposite film. Remarkably, following the incorporation of WME into the film containing 0.25% CNF, both the surface and cross-section of the film exhibited a striking smoothness. This phenomenon may be attributed to the robust binding interactions between the polyphenolic groups within WME and the

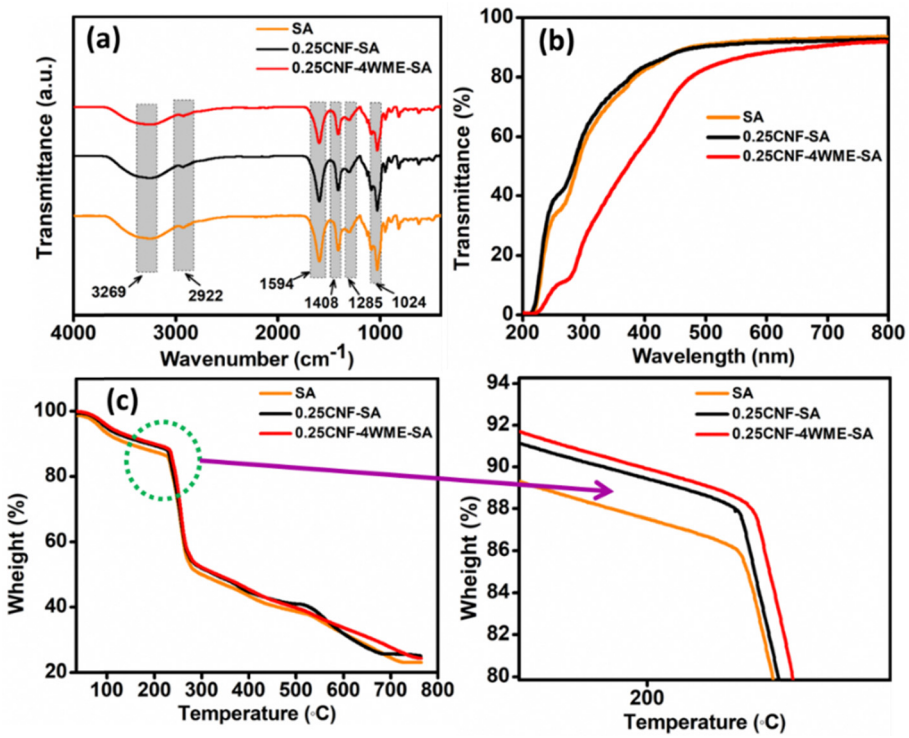

Fig. 2 (a)–(c) are the ATR FT-IR, UV and TGA spectra of SA, 0.25CNF-SA, and 0.25CNF-4WME-SA biopolymer film.

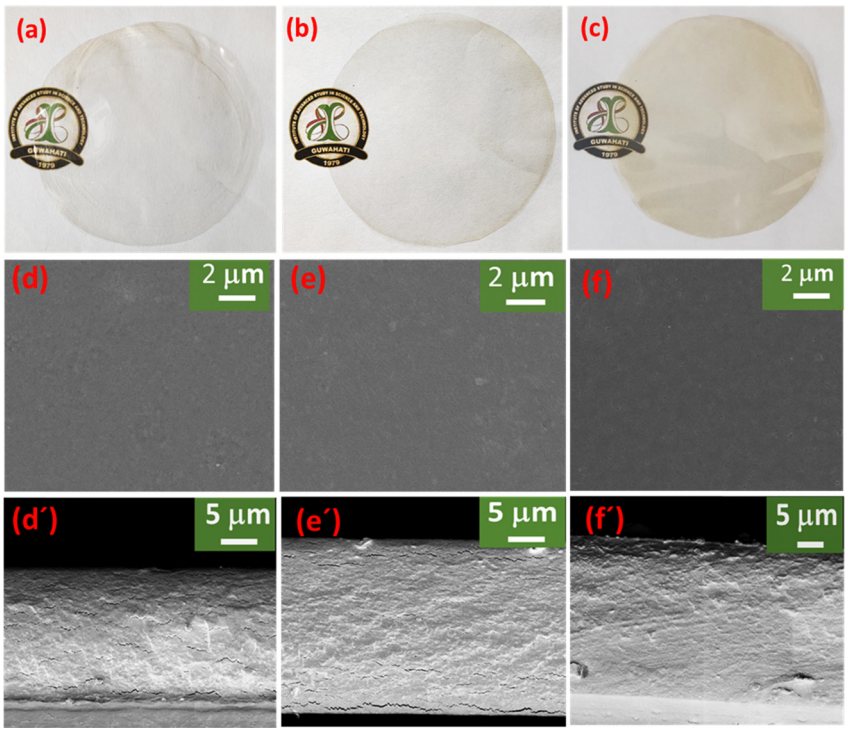

Fig. 3 (a)–(c) is the photograph of SA, 0.25CNF-SA, 0.25CNF-4WME-SA film; (d), (d′), (e), (e′), and (f), (f′) are the SEM surface and cross-section image of the SA, 0.25CNF-SA, 0.25CNF-4WME-SA film.

CNF, as well as the polymer chains of SA. A similar observation was also reported by Rahman *et al.*[15]

Initially, mechanical strength measurement was conducted on the pristine SA film and films incorporating various

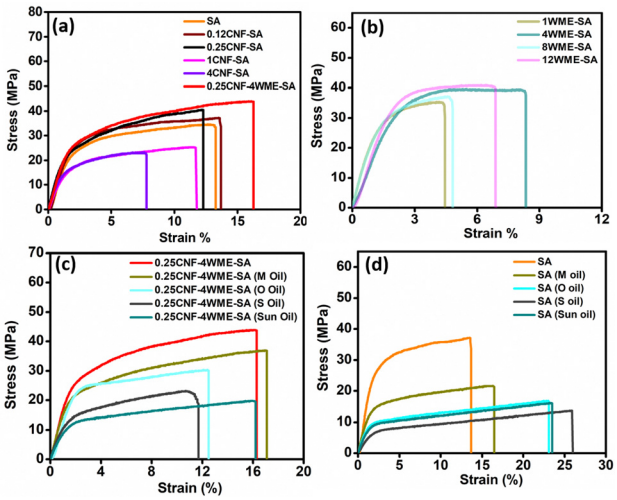

Fig. 4 (a) Stress *vs.* strain graph at the dry state of SA, 0.12CNF-SA, 0.25CNF-SA, 1CNF-SA, 4CNF-SA, and 0.25CNF-4WME-SA biopolymer film; (b) stress *vs.* strain graph at the dry state of 1MWE-SA, 4WME-SA, 8WME-SA, 12WME-SA; (c) stress *vs.* strain graph of 0.25CNF-4WME-SA biopolymer film after soaking at mustard oil, olive oil, soya bean oil, and sunflower oil; (d) stress *vs.* strain graph of SA biopolymer film after soaking at mustard oil, olive oil, soya bean oil, and sunflower oil.

concentrations of CNF *i.e.* 0.12CNF-SA, 0.25CNF-SA, 1CNF-SA, and 0.25CNF-4WME-SA film. This experiment was carried out to assess the acceptable CNF concentration for producing a film with outstanding mechanical properties that remain stable and suitable for packaging applications. The stress vs strain graph of the SA, 0.12CNF-SA, 0.25CNF-SA, 1CNF-SA, and 0.25CNF-4WME-SA film is given in Fig. 4(a), and the value of the Tensile strength, and % elongation is provided in Table 2. From the data, it is clear that with the blending of CNF into the SA films, the tensile strength of the nanocomposite film increases. However, the highest tensile strength was achieved by blending with 0.25% CNF (40.40 ± 2.50 MPa) among the pure SA film, 0.12%, 1% and 4% CNF blended film. The tensile strength was increased by 7.2% and 14.6% with blending of 0.12% and 0.25% CNF, respectively, as compared to the tensile strength of SA film. This might be due to the CNF with the fibrous structure and nanoscale dimension having high aspect ratios bonded intermolecular hydrogen bonding interaction with the polymeric chains of sodium alginate. Thus, a strong binding takes place in the 0.25% CNF as compared to the 0.12% CNF. Conversely, the percentage of elongation at break remained unchanged in the case of the 0.12% CNF film. However, in the 0.25% CNF blend film, the percentage of elongation at break decreased by 4.51% compared to the SA film.

This might be due to the stiffness of the CNF, which restricts the movements of the biopolymer matrix.

As the blending percentage of CNF increases by 1% and 4%, the tensile strength decreases by 33.04% and 26.66%, and the percentage of elongation at break also decreases by 41.75% and 12.03%, respectively, as compared to the pristine SA film. Upon increasing the concentration of CNF by more than 0.25%, a low binding of CNF with SA occurs due to the agglomeration of CNF in the biopolymer matrix. The agglomerations occur due to the addition of overloaded nanofibre into the SA.[15,40] Thus, phase separations and agglomerations at higher concentrated (1% and 4% CNF) CNF blended films were vividly observed in the SEM image as discussed above. However, incorporating the 4% WME in the 0.25CNF-SA film, there was an excellent binding interaction of nanofibre with the polyphenol groups of plant extract and the polymer chains of SA. Thus, there is no clump formation due to the proper binding, and an increment in tensile strength is 21.41%, as well as elongation, is 18.40% more than the pristine SA film. Therefore, 0.25CNF-4WME-SA fabricated film is a good choice for the packaging.

Table 2 Value of tensile strength, thickness, and elongation of SA, 0.25CNF-SA, 1CNF-SA, 4CNF-SA, and 0.25CNF-4WME-SA, 1WME-SA, 4WME-SA, 8WME-SA and 12WME-SA biopolymer film. (Data represented as mean ± standard deviation)

			Mechanical property	
S. no.	Sample name	Thickness (mm)	Tensile strength (MPa)	Elongation at break (%)
1	SA	0.042 ± 0.001	34.50 ± 2	13.30 ± 1.22
2	0.12CNF-SA	0.048 ± 0.0005	37.20 ± 1	13.60 ± 0.89
2	0.25CNF-SA	0.041 ± 0.0009	40.40 ± 2.50	12.30 ± 1.22
4	1CNF-SA	0.038 ± 0.0008	23.10 ± 1.60	7.77 ± 2.23
5	4CNF-SA	0.053 ± 0.0006	25.30 ± 1.80	11.70 ± 1.56
6	0.25CNF-4WME-SA	0.032 ± 0.001	43.90 ± 2	16.30 ± 3.22
7	1WME-SA	0.034 ± 0.0001	33.40 ± 1.50	4.45 ± 2.20
8	4WME-SA	0.025 ± 0.00002	38.20 ± 0.86	8.34 ± 1.56
9	8WME-SA	0.034 ± 0.00016	34.90 ± 2.12	4.82 ± 10
10	12WME-SA	0.053 ± 0.0004	39.60 ± 1.77	6.89 ± 1.25

5.2. Oil stability study of the biopolymer film

The material used for packaging edible oils must have stability in the respective oils. To check the stability of the composite film's 0.25CNF-4WME-SA and the pristine SA film, we perform mechanical measurements by soaking for 24 h in edible oils. The stress *vs.* strain graph for the SA and 0.25CNF-4WME-SA biopolymers films after soaking with mustard oil (M oil), olive oil (O oil), soybean oil (S oil), and sunflower oil (sun oil) is given in Fig. 4(d). The data are shown in Table 3. The 0.25CNF-4WME-SA film has an initial tensile strength of 43.90 MPa, and elongation of 16.30% in dry conditions (as shown in Table 3). After soaking in edible oils, the tensile strength of the biopolymer decreases. Mustard oil contains mainly linoleic acid (omega-6), and that does not affect the bonding interactions in the biopolymer chains and obtained quite stable in mechanical properties. However, in olive oil, there are particularly monounsaturated fatty acids (MUFA) like oleic acid, and they affect the mechanical properties to an extent. Due to the interactions of such MUFA with the SA biopolymer chains and weaken the bonding interactions between the polymeric chains. Similarly, soybean oils and sunflower oil also contain oleic acid. In sunflower oil, high oleic was present as compared to soyabean oil, as it contains a higher proportion of monosaturated. Therefore, biopolymer soaked in soyabean oil shows less decrease in mechanical strength than sunflower oil. In SA films soaked in the different edible oils, shows lower mechanical strength values

Table 3 Value of tensile strength, thickness, and elongation of SA, 0.25CNF-4WME-SA, 0.25CNF-4WME-SA (M oil), 0.25CNF-4WME-SA (O oil), 0.25CNF-4WME-SA (S oil), 0.25CNF-4WME-SA (sun oil), SA (M oil), SA (O oil), SA (S oil), SA (sun oil). (Data represented as mean ± standard deviation)

S. no.	Sample name	Thickness (mm)	Mechanical property	
			Tensile strength (MPa)	Elongation at break (%)
1	SA	0.042 ± 0.001	34.50 ± 2	13.30 ± 1.22
2	0.25CNF-4WME-SA	0.032 ± 0.001	43.90 ± 2	16.30 ± 3.22
3	0.25CNF-4WME-SA (M oil)	0.030 ± 0.002	36.70 ± 1.56	17.10 ± 2
4	0.25CNF-4WME-SA (O oil)	0.032 ± 0.092	29.70 ± 2.2	12.50 ± 1.2
5	0.25CNF-4WME-SA (S oil)	0.032 ± 0.001	21.60 ± 1.28	11.40 ± 1.56
6	0.25CNF-4WME-SA (sun oil)	0.032 ± 0.001	19.40 ± 1.15	14.90 ± 1.44
7	SA (M oil)	0.043 ± 0.002	21.20 ± 0.89	16.50 ± 1.58
8	SA (O oil)	0.038 ± 0.002	16.30 ± 2.10	21.20 ± 1.26
9	SA (S oil)	0.047 ± 0.001	13.40 ± 1.67	25.90 ± 2.23
10	SA (sun oil)	0.042 ± 0.001	16 ± 1.53	23.50 ± 1.88

than those of edible oil soaked 0.25CNF-4WME-SA biopolymer films (Table 3). This might be due to the presence of nanofiller, CNF in the 0.25CNF-4WME-SA films, can withstand the mechanical strength even after soaking in the different edible oils for 24 h. Thus, the 0.25CNF-4WME-SA film have stable in the different edible oils and is suitable for the packaging of edible oils.

5.3. Oil permeability

The oil permeability test was conducted on various edible oils, including mustard, olive, soybean, and sunflower oil using 0.25CNF-4WME-SA biopolymer films. The results revealed that no oil permeability was detected in the 0.25CNF-4WME-SA composite film. This indicates that the polymer chains are tightly bonded with the CNF within the polymer matrix, effectively preventing the oils from penetrating the biopolymer film. As a result, the 0.25CNF-4WME-SA nanocomposite film demonstrates its exceptional suitability for packaging edible oils.

5.4. Water vapour permeability (WVP)

WVP stands as a crucial parameter in packaging applications, serving as a valuable tool for assessing the movement of water vapour between food products and the surrounding environment through the packaging material. The WVP of SA, 0.25CNF-SA and 0.25CNF-4WME-SA biopolymer films are measured. The calculated value of WVP for SA, 0.25CNF-SA and 0.25CNF-4WME-SA films are 6.75×10^{-7}, 6.59×10^{-7} and 5.05×10^{-7}, respectively. The pristine SA film exhibited the highest WVP, which decreased upon the inclusion of CNF (0.25CNF-SA film). The lowest WVP value was achieved with the addition of WME (0.25CNF-4WME-SA film).

This outcome is attributed to the fact that in the SA film, water molecule absorption and diffusion predominantly take place on the film's surface, owing to the abundant presence of hydrophilic (–OH) groups on the SA film's surface.[41] The cellulose nanofibers, with their fibrous structure, in the 0.25CNF-SA film established interlocking hydrogen bonding interactions with the polymer chains, creating a tortuous path within the biopolymer matrix. Thus, the diffusion of water molecules through the nanocomposite film was reduced. While WME was incorporated into the biopolymer film, the polyphenols in the WME formed intermolecular hydrogen bonding interactions with the CNF and the polymeric chains of SA and increased the hydrophobic nature of the active film.[41] This leads to the form least water absorption on the film surface and improves the WVP property of the 0.25CNF-4WME-SA film.

5.5. GC–MS analysis of WME

From GC–MS data (Fig. 5), the table is tabulated in Table 4 for the compounds present and their area, % area. The percentage

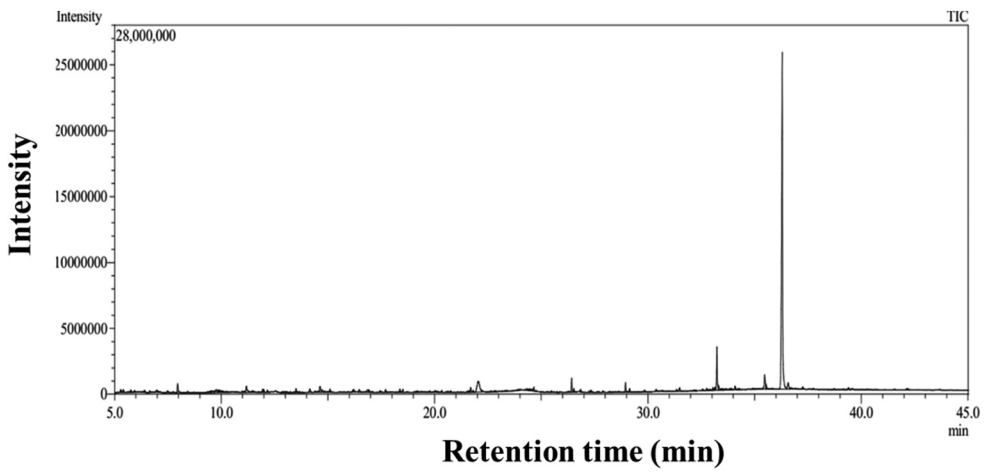

Fig. 5 GC–MS chromatographic profile of Moringa extract from water (WME).

Table 4 GC–MS spectral data for WME

Retention time	Major compounds	Molecular formula	Area %	Area
36.293	9-Octadecenamide, (*Z*)-	$C_{18}H_{35}NO$	46.41	25 561 246
33.229	Hexadecanoic acid, 2-hydroxy-1-(hydroxymethyl)ethyl ester	$C_{19}H_{38}O_4$	4.19	3 317 966
22.041	1,2,3,5-Cyclohexanetetrol, (1.alpha.,2.beta.,3.alpha.,5.beta.)-	$C_6H_{12}O_4$	3.82	7 187 281
35.472	Octadecanoic acid, 2,3-dihydroxypropyl ester	$C_{21}H_{42}O$	2.09	3 935 738
26.423	Hexadecanoic acid, methyl ester	$C_{17}H_{34}O_2$	1.15	2 165 351
7.955	Cyclohexanone	$C_6H_{10}O$	1.08	2 040 626
36.569	Octadecanamide	$C_{18}H_{37}NO$	1.07	2 019 662
11.176	(*R*,*S*)-2-Propyl-5-oxohexanal	$C_9H_{16}O_2$	1.02	1 921 437
28.948	Methyl stearate	$C_{19}H_{38}O_2$	0.8	1 509 676
14.629	Catechol	$C_6H_6O_2$	0.79	1 497 479
30.285	Benzyl.beta.-D-glucoside	$C_{13}H1_8O_6$	0.31	586 229

area represents the relative abundance of different compounds detected in the plant extract. There are several active compounds are present in the WME. Among them, the maximum % area is shown for 9-octadecenamide, (*Z*)- (an Oleamide), sometimes labelled as a fatty acid primary amide (FAPA). Hexadecanoic acid present in the WME is known as antioxidant property.[42] The componds present in the WME as determined from the GC–MS anlysis shows an excellent antioxidant property as reported in the earlier study.[43–52]

5.6. DPPH and ABTS free radical scavenging assay

Edible oils are easily oxidized and deteriorate due to lipid oxidations. The synthesis of antioxidant properties containing packaging materials can prevent the oxidation of the oils. Previous research reveals that packaging materials with antioxidant activity aids in preventing lipid oxidation by interfering with the activities that propagate radicals. Therefore, in this report, we perform the antioxidant test for WME and different percentages of WME blended SA film and WME-SA nanocomposite biopolymer film against DPPH· and ABTS· scavenging assay, and the results are shown in Table 5. The water extraction of plant compounds is a very easy and low-cost technique for large-scale production. Therefore, in this report, we used only water as a solvent for the extraction of the active compounds from the dried *Moringa Oleifera* leaves. A list of the predominant antioxidant compounds extracted from water (WME) is listed in Table 4. These have been demonstrated to have antioxidant properties in prior literature.[43–52] Generally, a greater yield in polyphenol extraction aligns with increased antioxidant activity, likely due to the combined effects of various substances present at varying concentrations and their strong ability to donate hydrogen atoms.[53] The WME shows very high free radical scavenging activity against both DPPH· (78.43%) and ABTS· (96.56%).

WME incorporated the 0.25CNF-SA film exclusively, primarily due to its outstanding mechanical properties when compared to the other CNF-containing films that were synthesized. The detailed mechanical properties of different percentages of CNF-composite films were discussed in the previous sections. In this study, we fabricated a range of WME-SA films by incorporating varying concentrations of dried WME, specifically 1%, 4%, 8%, and 12% (w/w) (with the total weight of SA), into the 0.25CNF-SA film. These films are denoted as 1WME-SA, 4WME-SA, 8WME-SA, and 12WME-SA, respectively. The details of synthesis were given in the experimental section. The DPPH· scavenging assay was conducted for the films 1WME-SA, 4WME-SA, 8WME-SA, 12WME-SA, and 0.25CNF-12WME-SA; the data is presented in Table 5. As the percentage of WME in the SA biopolymer increased from 1% to 12%, there was a noticeable rise in free radical scavenging activity against both DPPH· and ABTS. This increase can be primarily attributed to the growing presence of phenolic hydroxyl groups in the WME molecules, which enhances their ability to donate hydrogen atoms. Although we obtained the highest free radical scavenging property of the 8WME-SA and 12WME-SA, the mechanical stability of the film decreased due to the higher amount of the polyhenols content in the matrix. Thus 4% WME incorporated 0.25CNF-SA film i.e 0.25CNF-4WME-SA film exhibitaed excellent property. Interestingly, after incorporations of the CNF, the free radical scavenging property increases of the composite film in both the DPPH· and ABTS· assay as compared to the 4WME-SA film. This might be due to the CNF associated with the lignin, as discussed in the FT-IR spectra, and it increases the hydroxyl groups, thus providing the antioxidant property of the

Table 5 Results of antioxidant activity (DPPH· and ABTS· scavenging assay) of the plant extract and the fabricated biopolymer film. (Data represented as mean ± standard deviation)

S. no.	Sample name	Control absorbance	Volume of DPPH/ABTS (mL)	Volume of sample (mL)	% Scavenging assay	
					DPPH·	ABTS·
1	WME	0.779	4.0 mL	1.2 mL	78.43 ± 1.50	96.56 ± 2.10
2	1WME-SA				25.80 ± 1.66	29.04 ± 2.45
3	4WME-SA				32.09 ± 1.12	40.89 ± 2.55
4	8WME-SA				38.76 ± 2.10	59.76 ± 1.23
5	12WME-SA				40.94 ± 1.10	96.70 ± 1.76
6	0.25CNF-4WME-SA				41.33 ± 1.82	60.55 ± 1.98

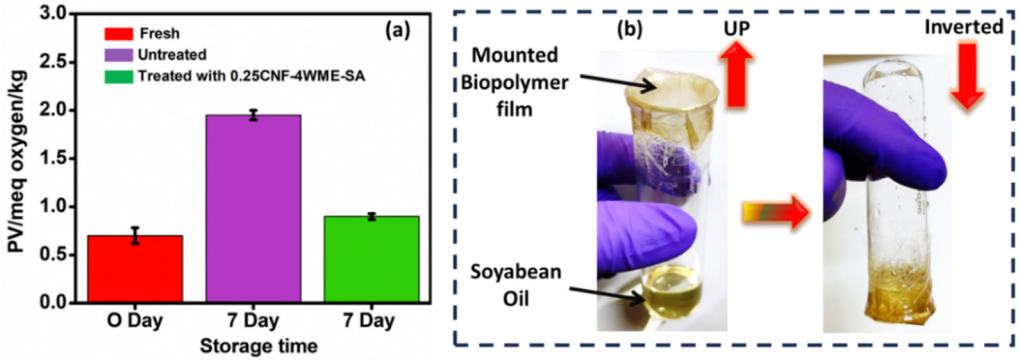

Fig. 6 (a) Graph representing peroxide value for soybean oil. (b) Schematic representation of soybean oil packaging for peroxide value determination.

biopolymer matrix after the incorporation of cellulose nanofiber. This result was in line with the earlier reported articles.[54,55] Thus, the 0.25CNF-4WME-SA shows the highest % scavenging assay and can be used for packaging edible oil to prevent their oxidation and increase their shelf life.

5.7. Practical applications of edible oil packaging

The scavenging property of the biopolymer film was investigated through peroxide value (PV) determinations to assess the generation of peroxides and hydroperoxides due to oxidative degradation. The value of the PV is displayed in a graph in Fig. 6(a). The experiment was performed by storing soybean oil for 7 days in an environmental chamber maintained at 50 ± 4 °C and 42 ± 2% relative humidity (RH). One sample was packed with the 0.25CNF-4WME-SA film, while another remained unpacked (without the film). Untreated soybean oil, after the same storage duration under the specified conditions, obtained a PV of (1.95 ± 0.05) mEq of oxygen per kg. Interestingly, with the packaging of the active biopolymer film, the PV of soybean oil decreased and was obtained at (0.9 ± 0.03) mEq of oxygen per kg. The PV was also determined for fresh soybean oil and was measured to be (0.7 ± 0.08) mEq of oxygen per kg. This suggests that the biopolymer film effectively mitigated the formation of peroxides and hydroperoxides in soybean oil during storage under oxidative conditions. This effect can be attributed to the presence of antioxidant compounds within the film.[4] Therefore, the 0.25CNF-4WME-SA film can be used as an active packaging material to enhance the shelf life of soyabean oil.

5.8. Cell viability study

Assessing the toxicity of the newly developed material intended for use in packaging applications is essential. The liver is the largest organ in the body and plays a crucial role in the removal of xenobiotic compounds. Therefore, hepatocytes or liver cells are the primary focus of toxicity studies. Moreover, liver cells are more prone to chemical interactions. Hence, the film samples' cytotoxicity was evaluated using CC1 hepatocyte cells as an *in vitro* model. Fig. 7(e) illustrates the percentage of cell viability at 125 μg mL^{-1} for SA, 0.25CNF-SA, 0.25CNF-4WME-SA, and the control group. The results indicate that cell viability for all samples exceeded 95%, demonstrating the safety of the prepared films for practical use. Light microscope images of the cells after 24 h of treatment are presented in Fig. 7(a)–(d).

In this investigation, the 24 h treatment of CC1 hepatocytes with 125 μg mL^{-1} of SA, 0.25CNF-SA, and 0.25CNF-4WME-SA revealed no toxic effects. The treated groups exhibited cuboidal cell morphology, intact cell membrane integrity, and centrally placed ovoid nuclei, closely resembling the non-treated control group. This observation emphasizes the non-toxic nature of the developed films.

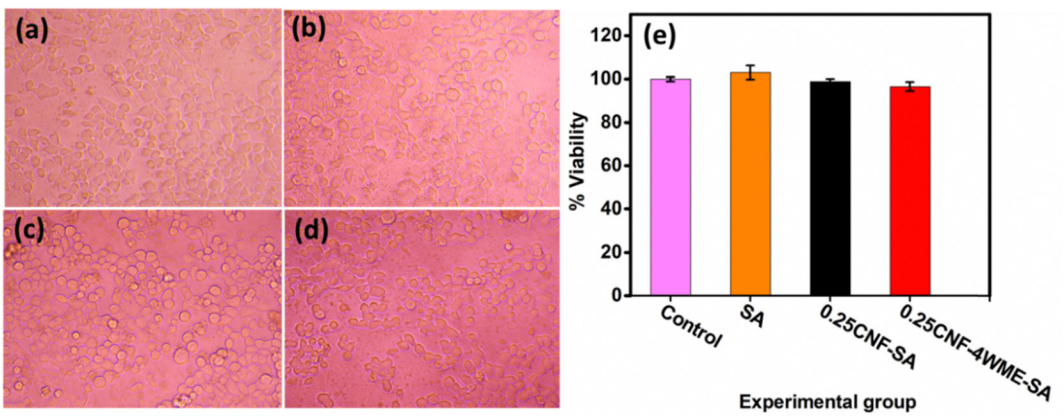

Fig. 7 Light microscopy images of CC1 hepatocyte cells treated with (a) control (b) SA (c) 0.25CNF-SA (d) 0.25CNF-4WME-SA, and (e) graph represent the percent of viability of the samples toward CC1 hepatocytes cell line treated after 24 h.

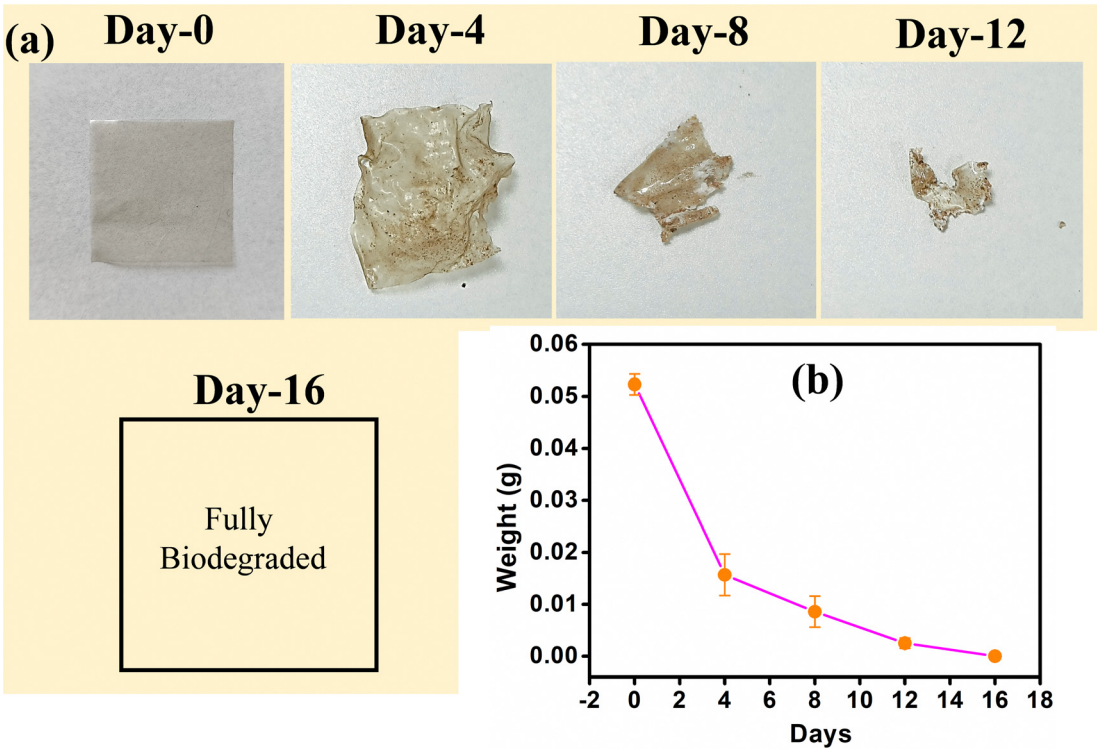

Fig. 8 (a) Photographs of 0.25CNF-4WME-SA film during biodegradable test. (b) Changes of weight during biodegradation 0.25CNF-4WME-SA film.

5.9. Biodegradability test

The biodegradability experiment was conducted on the 0.25CNF-4WME-SA film to assess its degradation behaviour in soil. The physical appearance of the film throughout the experiment is shown in Fig. 8. The study was conducted over a period of 16 days, during which the film completely degraded in the soil. Initially, the biopolymer film had a weight of (0.0523 ± 0.002) g. Throughout the experiment, the film's weight steadily decreased, as shown in Fig. 8(b). By days 4, 6, and 12, the recorded weights were (0.0157 ± 0.004) g, (0.0086 ± 0.003) g, and (0.0025 ± 0.001) g, respectively. The weight loss of the nanocomposite film is attributed to the breakdown of polymer chains into smaller molecular fragments, driven by abiotic factors like oxidation and hydrolysis, as well as biotic processes involving bacteria in the soil.[15] Based on this biodegradation study, it can be concluded that the fabricated 0.25CNF-4WME-SA film is fully biodegradable within 16 days of burial in soil. Slezak *et al.* demonstrated that polylactide (PLA) combined with polybutylene succinate and a mineral filler was biodegradable, taking approximately 12 months to degrade under natural conditions.[56] Therefore, the fabricated 0.25CNF-4WME-SA film exhibits greater degradability compared to commercially used PLA.

6. Conclusion

In summary, in this work, we successfully fabricate cellulose nanofiber-moringa plant extract-sodium alginate composite film. The fabricated nanocomposite was synthesized using a solvent-casting technique. The fabricated nanocomposite film shows good antioxidant properties that are required to enhance the shelf life of edible oils. The cellulose nanofiber-moringa plant extract-sodium alginate composite film shows higher mechanical strength and is a good choice for packaging applications. The CNF was derived from arjuna plant fruits through an acid hydrolysis process, while the antioxidant compounds (WME) were extracted from *Moringa oleifera* leaves using water as a solvent. The fabricated film absorbs UV light and can provide a UV shield property. Moreover, it exhibited resilience to high temperatures, withstanding up to ~230 °C. The film proved oil-stable and, preventing oil penetration and controlling leakage. A practical application of edible oil packaging was successfully demonstrated, showcasing the effective free radical scavenging property of the active biopolymer film. The fabricated films tested the toxicity effect by an *in vitro* model on CC1 hepatocyte cells, which confirms that the films are non-toxic. The fabricated 0.25CNF-4WME-SA composite biopolymer film emerges as a promising material capable of replacing traditional petroleum-based polymers. It holds potential as a preferred choice for active edible oils packaging, effectively contributing to the enhancement of their shelf life.

Data availability

The datasets used and/or analyzed during the current study available from the corresponding author on reasonable request.

Conflicts of interest

There are no conflicts to declare.

Acknowledgements

The authors want to thank IASST for the in-house project. The authors would like to thank SAIC, IASST for the instrumentation facility. S. R. would like to acknowledge DST, New Delhi, for the INSPIRE Fellowship. S. R. also thanks Mr Bitopan Boro for his valuable help.

References

1 M. Holler, J. Alberdi-Cedeño, A. Auñon-Lopez, T. Pointner, A. Martínez-Yusta, J. König and M. Pignitter, *Food Packag. Shelf Life*, 2023, **36**, 101051.
2 M. S. Tawfik and A. Huyghebaert, *Food Chem.*, 1999, **64**, 451–459.
3 A. E. El-Hadary and M. Taha, *Food Sci. Nutr.*, 2020, **8**, 1798–1811.
4 R. Rashid, S. M. Wani, S. Manzoor, F. A. Masoodi and M. M. Dar, *Food Biosci.*, 2022, **49**, 101917.
5 T. Tshabalala, A. R. Ndhlala, B. Ncube, H. A. Abdelgadir and J. Van Staden, *S. Afr. J. Bot.*, 2020, **129**, 106–112.
6 N. Z. Abd Rani, K. Husain and E. Kumolosasi, *Front. Pharmacol.*, 2018, **9**, 108.
7 A. Fatiqin, H. Amrulloh, I. Apriani, A. Lestari, B. Erawanti, A. Saputri, M. Gita, M. Fitrianti, R. R. Sathuluri, Y. S. Kurniawan, Rr. M. S. Wulan and M. S. Khan, *Indones. J Nat. Pigm.*, 2021, **3**, 43.
8 N. Flórez, E. Conde and H. Domínguez, *J. Chem. Technol. Biotechnol.*, 2014, **90**, 590–607.
9 G. Barzan, A. Sacco, A. M. Giovannozzi, C. Portesi, C. Schiavone, J. Salafranca, M. Wrona, C. Nerín and A. M. Rossi, *Food Chem.*, 2024, **432**, 137088.
10 R. Nisticò, *Polym. Test.*, 2020, **90**, 106707.
11 S. Rahman, J. Gogoi, S. Dubey and D. Chowdhury, *Int. J. Biol. Macromol.*, 2024, **255**, 128197.
12 S. Rahman, A. Konwar, G. Majumdar and D. Chowdhury, *Carbohydr. Polym. Technol. Appl.*, 2021, **2**, 100158.
13 K. Z. Elwakeel, A. M. Daher, A. I. L. A. El-Fatah, H. A. E. Monem and M. M. H. Khalil, *J. Dispersion Sci. Technol.*, 2016, **38**, 145–151.
14 S. Rahman and D. Chowdhury, *Int. J. Biol. Macromol.*, 2022, **216**, 571–582.
15 S. Rahman, A. Konwar, G. Gogoi and D. Chowdhury, *ACS Sustainable Chem. Eng.*, 2023, **12**, 795–815.
16 S. Rahman, A. Konwar, A. N. Konwar, S. Dubey, M. P. Ghosh, B. Boro, D. Thakur and D. Chowdhury, *Biomacromolecules*, 2024, **25**, 1491–1508.
17 Y. Lei, Q. Yao, Z. Jin and Y.-C. Wang, *Food Chem.*, 2023, **404**, 134528.
18 S. Sepahvand, A. Ashori and M. Jonoobi, *Int. J. Biol. Macromol.*, 2023, **244**, 125344.
19 H. Shaghaleh, X. Xu and S. Wang, *RSC Adv.*, 2018, **8**, 825–842.
20 M. Prakash Menon, R. Selvakumar, P. Suresh Kumar and S. Ramakrishna, *RSC Adv.*, 2017, **7**, 42750–42773.
21 Q.-F. Guan, H.-B. Yang, Z.-M. Han, Z.-C. Ling, K.-P. Yang, C.-H. Yin and S.-H. Yu, *Nano Lett.*, 2021, **21**, 8999–9004.
22 J. Singh, S. Kumar, B. Rathi, K. Bhrara and B. S. Chhikara, *J. Mater. NanoSci.*, 2015, **2**(1), 1–7.
23 A. B. Choudhari, S. Nazim, P. V. Gomase, A. S. Khairnar, A. Shaikh and P. Choudhari, *J. Pharma Res.*, 2011, **4**(3), 580–581.
24 M. Zannat and U. Kulsum, *Chemical and biochemical studies on the fruit of arjun tree (terminalia arjun linn)*, 2003.
25 V. K. Singh and N. Soni, *Trends Appl. Sci. Res.*, 2019, **14**, 233–242.
26 P. Das, S. Ganguly, S. R. Ahmed, M. Sherazee, S. Margel, A. Gedanken, S. Srinivasan and A. R. Rajabzadeh, *ACS Appl. Polym. Mater.*, 2022, **4**, 9323–9340.
27 T. Bhattacharjee, S. Rahman, D. Deka, M. K. Purkait, D. Chowdhury and G. Majumdar, *Mater. Chem. Phys.*, 2022, **288**, 126413.
28 S. Tanpichai, S. K. Biswas, S. Witayakran and H. Yano, *ACS Sustainable Chem. Eng.*, 2019, **7**, 18884–18893.
29 H. Ren, Z. Xu, C. Du, Z. Ling, W. Yang, L. Pan, Y. Tian, W. Fan and Y. Zheng, *Int. J. Biol. Macromol.*, 2023, **242**, 124938.
30 B. Wang and D. Li, *Composites, Part A*, 2015, **79**, 1–7.
31 H. Tibolla, F. M. Pelissari, J. T. Martins, A. A. Vicente and F. C. Menegalli, *Food Hydrocolloids*, 2018, **75**, 192–201.
32 Y. Zhao, C. Moser, M. E. Lindström, G. Henriksson and J. Li, *ACS Appl. Mater. Interfaces*, 2017, **9**, 13508–13519.
33 H. Khalili, A. Bahloul, E.-H. Ablouh, H. Sehaqui, Z. Kassab, F.-Z. Semlali Aouragh Hassani and M. El Achaby, *Int. J. Biol. Macromol.*, 2023, **226**, 345–356.
34 M. Kuczajowska-Zadrożna, U. Filipkowska and T. Jóźwiak, *J. Environ. Chem. Eng.*, 2020, **8**, 103878.
35 W. Janik, M. Nowotarski, K. Ledniowska, D. Y. Shyntum, K. Krukiewicz, R. Turczyn, E. Sabura, S. Furgoł, S. Kudła and G. Dudek, *Sci. Rep.*, 2023, **1**, 13.
36 A. Kumawat, K. Jasuja and C. Ghoroi, *ACS Appl. Bio Mater.*, 2023, **6**, 4111–4126.
37 S. Roy, R. Chawla, R. Santhosh, R. Thakur, P. Sarkar and W. Zhang, *Trends Food Sci. Technol.*, 2023, **141**, 104198.
38 X. Wang, J. Cong, L. Zhang, Z. Han, X. Jiang and L. Yu, *J. Agric. Food Chem.*, 2023, **71**, 15352–15362.
39 L. Zhang, K. Chen and Y. Wu, *ACS Sustainable Chem. Eng.*, 2019, **7**, 15238–15246.
40 N. Jamaluddin, T. Kanno, T.-A. Asoh and H. Uyama, *Mater. Today Commun.*, 2019, **21**, 100587.
41 V. G. Bhat, S. S. Narasagoudr, S. P. Masti, R. B. Chougale, A. B. Vantamuri and D. Kasai, *Int. J. Biol. Macromol.*, 2022, **200**, 50–60.
42 S. Siswadi and G. S. Saragih, *AIP Conf. Proc.*, 2021, **2353**, 030098.
43 O. C. Atewolara-Odule, *et al.*, Antibacterial and antioxidant activities of the essential oil from Nauclea latifolia (Smith) leaves Ife, *J. Food Sci. Technol.*, 2020, **4**(1), 73–83.
44 B. Benzidia, M. Barbouchi, H. Hammouch, N. Belahbib, M. Zouarhi, H. Erramli, N. Ait Daoud, N. Badrane and N. Hajjaji, *J. King Saud Univ., Sci.*, 2019, **31**, 1175–1181.

45 V. Ragupathi, *et al.*, Antibacterial activity, in vitro antioxidant potential and gc-MS characterization of methanolic extract of Gymnopilus junonius, a wild mushroom from Southern Western Ghats, India, *Eur. J. Biomed.*, 2018, **5**, 650–657.
46 J. Rani and M. Kapoor, Gas chromatography-mass spectrometric analysis and identification of bioactive constituents of Catharanthus roseus and its antioxidant activity, *Gas*, 2019, **12**(3), 461–465.
47 M. P. Rivas Romero, R. Estévez Brito, J. M. Rodríguez Mellado, J. González-Rodríguez, M. Ruiz Montoya and R. Rodríguez-Amaro, *LWT*, 2018, **95**, 157–166.
48 M. Davoodbasha, B. Edachery, T. Nooruddin, S.-Y. Lee and J.-W. Kim, *Microb. Pathog.*, 2018, **115**, 233–238.
49 R. Ritmaleni, R. B. Fatmayanti, S. D. Ekananda, B. N. Tranggono, N. K. Arsani and R. Rumiyati, *Indones. J. Pharm.*, 2023, **34**(1), 93–102.
50 F. Khabbaz, A.-C. Albertsson and S. Karlsson, *Polym. Degrad. Stab.*, 1999, **63**, 127–138.
51 M. Dawood Shah, J. Seelan Sathiya Seelan and M. Iqbal, *Arabian J. Chem.*, 2020, **13**, 7170–7182.
52 I. V. Smolyaninov, O. V. Pitikova, E. O. Korchagina, A. I. Poddel'sky, G. K. Fukin, S. A. Luzhnova, A. M. Tichkomirov, E. N. Ponomareva and N. T. Berberova, *Bioorg. Chem.*, 2019, **89**, 103003.
53 P. Siddhuraju and K. Becker, *J. Agric. Food Chem.*, 2003, **51**, 2144–2155.
54 L. V. Hai, L. Zhai, H. C. Kim, P. S. Panicker, D. H. Pham and J. Kim, *Nanomaterials*, 2020, **10**, 1752.
55 Y. He, H.-C. Ye, T.-T. You and F. Xu, *Food Hydrocolloids*, 2023, **137**, 108355.
56 R. Slezak, L. Krzystek, M. Puchalski, I. Krucińska and A. Sitarski, *Sci. Total Environ.*, 2023, **866**, 161401.